Biophysical and Pharmacological Characterization of $K_V7.4$ Channels Using Automated Patch Clamp

Kim Boddum, Pietro Scaduto, Anissa Bara, Naja Møller Sørensen

Sophion Bioscience A/S
Industriparken 39
2750 Ballerup, Denmark

Introduction

The K_V7 family of voltage-gated potassium channels plays critical roles in cellular excitability and signal regulation. Among them, $K_V7.4$ channels are specifically expressed in the inner ear and are crucial for auditory function. Dysfunction or modulation of these channels has been linked to epilepsy and age-related hearing loss. Modulating $K_V7.4$ channels provides therapeutic opportunities, with activators shown to stabilize electrical activity and protect hearing. Using the Sophion QPatch automated patch clamp (APC) platform, we developed a robust and reproducible assay for $K_V7.4$ biophysical characterization and pharmacological testing. This work highlights the platform's ability to support high-quality, high-throughput compound screening.

Conclusion

The QPatch platform demonstrated high assay success rates (71% ± 6%) and precise biophysical characterization of $K_V7.4$ channels. Retigabine, an activator, shifted voltage-dependent activation and tail currents, highlighting the assay's sensitivity to pharmacological modulation. Biophysical properties, including voltage sensitivity ($V_{½}$) and current amplitudes, were reproducibly assessed, supporting reliable compound evaluation. This assay facilitates the study of $K_V7.4$ modulators for therapeutic applications, addressing unmet needs in epilepsy, hearing loss, and other neurological disorders. The platform's efficiency and reliability position it as a valuable tool in ion channel research and drug discovery.

Material and methods

HEK-$K_V7.4$ cells, provided by Saniona, were cultured per supplier protocols. Experiments were conducted at 22°C ± 1°C using QPatch II and single-hole consumables. Key biophysical parameters, such as voltage-dependent currents, conductance-voltage relationships, and tail currents, were measured using Sophion analyzer software. Pharmacological assessments included activators like retigabine and inhibitors like linopirdine, profiling their effects on voltage sensitivity, gating kinetics, and current amplitude. Concentration-response curves were generated to determine EC_{50} and IC_{50} values.

Results

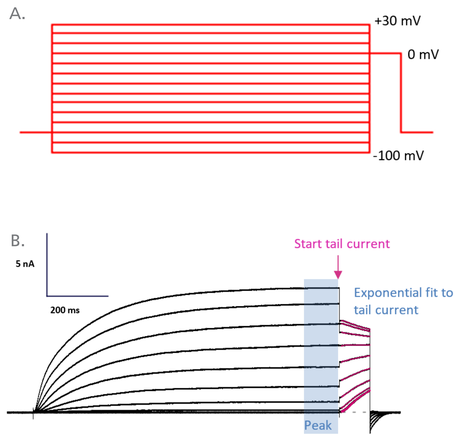

Fig. 1: Evaluation of $K_V7.4$ currents on QPatch. **A)** Voltage protocol applied for biophysical evaluation of $K_V7.4$ channels. **B)** Representative $K_V7.4$ currents in response to a step protocol of 1s long with, +10 mV increment steps from -100 mV to +30 mV (activation peak, blue cursor), followed by a 100 ms step to -10 mV (tail current).

Table 1: Group statistics on the Biophysical properties of $K_V7.4$. Shown values are average values ± SD.

Biophysical properties	Avg. ± SD
Well QC pass rate (%)	71% ± 6
Peak current at 20 mV (nA, fig. 1)	3.6 ± 0.3
$V_{½}$ (peak current, mV, fig. 3)	-25.3 ± 1.0
V_{Rev} (mV, fig. 3)	-42.9 ± 0.8
$V_{½}$ tail (mV, fig. 5)	-19.5 ± 1.4
Lidocaine	>100
Phenytoin	>100

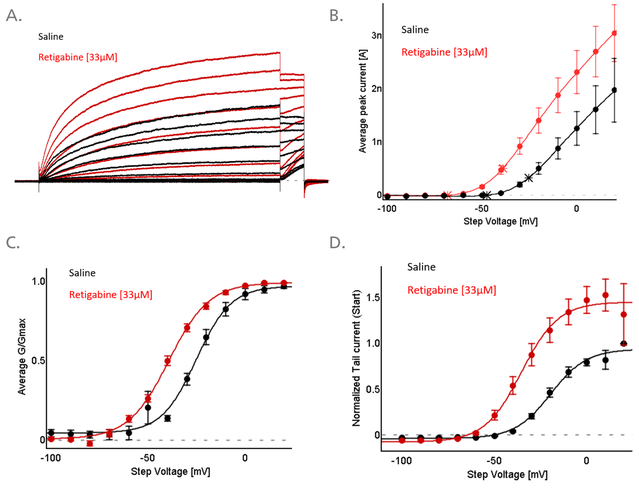

Fig. 2: Pharmacological modulation of $K_V7.4$ biophysics by retigabine. **A)** Representative $K_V7.4$ current traces under saline conditions (black) and after application of 33 µM retigabine (red). **B)** Average current from the last 50 ms of the activation step plotted against voltage, showing the voltage-dependent activation of the $K_V7.4$ channel in saline (black, n=14) and retigabine (red, n=14) conditions. $V_{½}$ and V_{Rev} are indicated with stars on both curves. **C)** Relative conductance (normalized within each cell to max conductance) plotted against voltage in saline (black) and in the presence of retigabine (red). **D)** Tail current-voltage relationship with (red) and without (black) retigabine. Error bars represent mean values +/- SD. The fitted curves represent standard (Fig 2B) or transformed (Fig. 2C-D) Boltzmann fits.

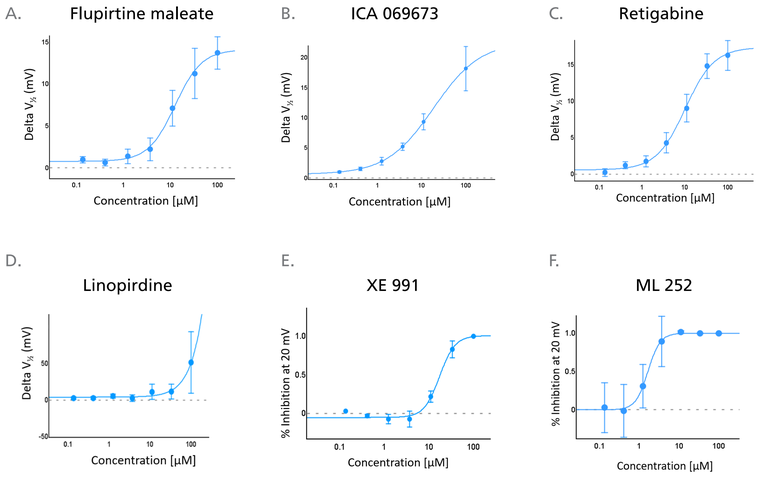

Fig. 3: Pharmacological evaluation of reference compound profiles on $K_V7.4$ channels. Cumulative concentration-response curves representing [Delta $V_{½}$] for $K_V7.4$ activators flupirtine maleate **(A)**, ICA 069673 **(B)**, and retigabine **(C)**. Effects of $K_V7.4$ inhibitors such as linopirdine **(D)**, XE 991 dihydrochloride **(E)** and ML 252 **(F)** are represented by cumulative concentration-response curves plotting the current amplitude at +20 mV.

Table 2: Summary table showing EC_{50} values from fig. 3A-C.

	EC_{50} for [Delta $V_{½}$]	EC_{50} for I_{-40mV}
Flupirtine maleate	12.6 µM	15.9 µM
ICA 069673	18.7 µM	8.9 µM
Retigabine	10.3 µM	9.5 µM

Table 3: Summary table showing IC_{50} values from fig. 3D-F

	EC_{50} for [Delta $V_{½}$]	IC_{50} for I_{-20mV}
Linopirdine	> 30 µM	5.1 µM
ML 252	> 30 µM	1.5 µM
XE 991	> 30 µM	14.4 µM

Presented @BPS2025